Title: Host immune responses after suprachoroidal delivery of AAV8 in nonhuman primate eyes.

Authors; Sook Hyun Chung[1], Iris Natalie Mollhoff[1], Alaknanda Mishra[2], Tzu-Ni Sin[1], Taylor Ngo[1], Thomas Ciulla[3], Paul Sieving[1], Sara M. Thomasy[1,4], and Glenn Yiu[1].

1. Department of Ophthalmology & Vision Science, University of California Davis, Davis, CA, U.S.A.
2. Department of Cell Biology & Human Anatomy, University of California Davis, Davis, CA, U.S.A.
3. Clearside Biomedical Inc, Alpharetta, GA, U.S.A
4. Department of Surgical and Radiological Sciences, School of Veterinary Medicine, University of California Davis, Davis, CA, U.S.A.

Correspondence should be addressed to G.Y (gyiu@ucdavis.edu).

Corresponding author

Glenn Yiu, M.D., PhD.

Department of Ophthalmology & Vision Science

University of California Davis

Email: gyiu@ucdavis.edu

21 Phone: +1 (916) 734-6602

22 Address: 4860 Y St., Suite 2400 Sacramento, CA, 95817

23

24 Short title: Immune response after intraocular AAV8 delivery

25

Abstract (200 words)

The suprachoroid is a potential space located between the sclera and choroid of the eye which provides a novel route for ocular drug or viral vector delivery. Suprachoroidal injection of AAV8 using transscleral microneedles enables widespread transgene expression in eyes of nonhuman primates, but may cause intraocular inflammation. We characterized the host humoral and cellular immune responses after suprachoroidal delivery of AAV8 expressing green fluorescent protein (GFP) in rhesus macaques, and found that it can induce a mild chorioretinitis that resolves after systemic corticosteroid administration, with recovery of photoreceptor morphology but persistent immune cell infiltration after 3 months. Suprachoroidal AAV8 triggered B-cell and T-cell responses against GFP, but only mild antibody responses to the viral capsid as compared to intravitreal injections of the same vector and dose. Systemic biodistribution studies showed lower AAV8 levels in liver and spleen after suprachoroidal injection compared with intravitreal delivery. Our findings suggest that suprachoroidal AAV8 primarily triggers host immune responses to GFP, likely due to sustained transgene expression in scleral fibroblasts outside the blood-retinal barrier, but elicits less humoral immune reactivity to the viral capsid than intravitreal delivery due to lower egress into systemic circulation. Thus, suprachoroidal AAV delivery of human transgenes may have significant translational potential for retinal gene therapy.

Introduction

The first approved ocular gene therapy for treating biallelic RPE65 mutation-associated retinal dystrophy, Leber's Congenital Amaurosis, has generated much enthusiasm for the use of adeno-associated viruses (AAVs) as vectors for retinal gene delivery.[1–6] Recombinant AAVs are highly effective vectors for gene delivery due to their ability to transduce a wide variety of retinal cell types and relative safety given their nonpathogenic and non-integrating nature.[7] However, although AAV vectors are much less immunogenic than adenoviruses, host immune responses triggered by the viral vector or transgene product can limit the effectiveness of the treatment.[8,9] Humoral immune responses from neutralizing antibodies (NAbs) produced by B-cells can inhibit vector transduction. These antibodies may arise from prior exposure to wild-type AAV causing pre-existing immunity, or be triggered by therapeutic vector administration which prevents or suppresses further transduction.[10–13] Also, cell-mediated immune responses from cytokine-secreting T-cells can directly destroy transduced cells.[14] Together, host humoral and cellular immune responses contribute to eliminating vectors and transduced cells, thus limiting the therapeutic effect.

Although the eye has been considered to be an immunologically-protected space,[15] the immunogenicity of AAV-mediated gene transfer in the eye varies with the route of administration. Subretinal injections, which entail a needle puncture through the neurosensory retina, enables efficient transduction of multiple cell types including photoreceptors and the underlying retinal pigment epithelium (RPE), and triggers minimal humoral immune responses.[16,17] However, the procedure requires complex vitrectomy surgery and the therapeutic effect is limited to the area of the injected fluid bleb. Intravitreal injections can be easily performed in an outpatient clinical setting, and newer generations of AAV can overcome the internal limiting membrane (ILM)

barrier to transduce deeper retinal layers.[18,19] But unlike subretinal injections, intravitreal delivery triggers more pronounced humoral and cellular responses against the AAV capsid, occasionally to levels matching systemic administration.[13,20]

We and others have recently described a novel mode of ocular gene delivery by injecting AAV into the suprachoroidal space, which is located between the scleral wall and the choroidal vasculature of the eye.[21,22] Although this potential space is barely detectable under physiologic conditions,[23,24] suprachoroidal injection of compounds using transscleral microneedles expands the suprachoroidal space as seen on *in vivo* imaging,[25,26] enabling targeted drug delivery to retinal and choroidal tissues while minimizing adverse effects on anterior segment structures.[27–31] Suprachoroidal injection of a triamcinolone acetonide suspension using these microneedles has been effective in treating macular edema from noninfectious uveitis in human clinical trials.[32]

Using nonhuman primates (NHPs), we found that suprachoroidal injection of AAV8 using transscleral microneedles enables widespread, peripheral transduction of mostly RPE cells. By contrast, subretinal injection of AAV8 transduced outer retinal cells including photoreceptors and RPEs, but was limited to the injection site.[21] Since the suprachoroidal space is located outside the blood-retinal barrier, we also investigated the inflammatory response in retinal and choroidal tissues, and found a greater degree of local immune cell infiltration after suprachoroidal delivery of AAV8 compared with subretinal or intravitreal injections. Interestingly, we found that intravitreal AAV8 triggered more serum NAbs than the other modes of injection, likely due to differences in the pharmacokinetics and biodistribution of the different modes of ocular AAV delivery.

In this ancillary study, we explore in detail the host humoral and cellular immune responses to suprachoroidal AAV8 in these rhesus macaques. Like humans, NHPs are natural hosts for wild-

type AAV and develop immune conversions to subclinical infection, making them an excellent animal model for predicting host immune responses to AAV vectors in humans. We found that suprachoroidal injection of AAV8 expressing green fluorescent protein (GFP) can elicit a transient chorioretinitis that clinically resolves after systemic corticosteroid administration, with recovery of photoreceptor morphology despite some persistence of immune cell infiltration over 3 months. Suprachoroidal injections trigger both B-cell and T-cell responses against the GFP transgene product, whereas the response against AAV8 capsid was minimal compared with intravitreal injections. Systemic biodistribution assays showed limited presence of the AAV8 in the liver and spleen after suprachoroidal injections as compared with intravitreal delivery. As suprachoroidal injection of AAV is currently under evaluation for retinal gene therapy in human clinical trials, our results provide an important, clinically-relevant, and unique exploration of host immune responses from viral gene delivery to different ocular compartments surrounding the blood-retinal barrier.

Results

Study design and clinical course

Experiments to evaluate the transduction efficacy, pattern, durability, and cell-type specificity of suprachoroidal AAV8 injections in rhesus macaques using transscleral microneedles have been previously described.[21] Briefly, we identified 5 animals between age 4-10 years with no pre-existing NAbs against AAV8, and injected both eyes with NHP-grade AAV8 that expresses enhanced GFP under a cytomegalovirus (CMV) promoter at 7×10^{11} vg/eye (low dose) or 7×10^{12} vg/eye (high dose), using either a 700-μm long 30-gauge microneedle (Clearside Biomedical, Alpharetta, GA, USA) for suprachoroidal or transscleral subretinal injection, or a 0.5-inch-long 30-gauge conventional needle for intravitreal injection (Supplementary Table 1). Of these, two

113 animals received suprachoroidal AAV8 in both eyes (Rhesus 01 with 7 x 10^{11} vg/eye and Rhesus
114 02 with 7 x 10^{12} vg/eye), two animals (Rhesus 03 and 04) received suprachoroidal injection of
115 AAV8 in one eye (7 x 10^{12} vg/eye) and subretinal delivery of AAV8 in the contralateral eye (7 x
116 10^{12} vg/eye), and the last animal (Rhesus 05) received intravitreal injection of AAV8 in both eyes
117 (7 x 10^{12} vg/eye). After 1 month, suprachoroidal delivery of high-dose AAV8 produced diffuse,
118 peripheral, and circumferential GFP fluorescence with a punctate pattern of expression (Figure
119 1A). By comparison, subretinal AAV8 resulted in a focal area of intense GFP expression (Figure
120 1B), while intravitreal AAV8 only produced a small peripapillary area of faint expression at the
121 same high dose (Figure 1C). Suprachoroidal delivery of low-dose AAV8 (7 x 10^{11} vg/eye) did not
122 produce any detectable transgene expression on fundus fluorescence imaging.

123 Although most of the animals did not exhibit significant anterior chamber (AC) or vitreous
124 inflammation throughout the study, Rhesus 02 developed mild 2+ AC cell based on
125 Standardization of Uveitis Nomenclature (SUN) criteria at 2 weeks requiring treatment with oral
126 prednisone (1 mg/kg) for 2 weeks with subsequent resolution of the AC cell by month 1. At 1
127 month, this animal also demonstrated a peripheral chorioretinitis with small, punctate spots (Figure
128 1D), some perivascular sheathing (Figure 1E), and radial retinal striae in the macular region
129 without significant macular edema (Figure 1F), which all appear resolved by month 3 (Figures 1G-
130 1I). Spectral domain-optical coherence tomography (SD-OCT) imaging showed fine,
131 hyperreflective foci in the vitreous and retinal surface at 1 month (Figure 1J) indicating subclinical
132 vitritis not readily seen on funduscopic examination, which also resolved after 3 months (Figure
133 1K). We did not note significant vitreous cell in the peripheral regions of the transduced retina in
134 Rhesus 02, or in any other animals after suprachoroidal delivery of AAV (Figure 1L). Eyes that
135 received subretinal AAV8 showed localized vascular dilation and perivascular hyperreflective foci

in the vitreous in the most intense regions of GFP expression (Figure 1M and 1O), indicating localized vasculitis and subclinical vitritis in these animals. Eyes that received intravitreal injection of AAV8 showed no detectable vitritis, chorioretinitis, or vasculitis, even in the small peripapillary region of transduction (Figures 1N and 1P). Thus, suprachoroidal injection of AAV8 may trigger an anterior uveitis, peripheral chorioretinitis, and mild vitritis that all resolve with oral corticosteroid treatment over 2 weeks. Subretinal AAV8 can also trigger mild, localized vasculitis and vitritis in the area of transduction, while intravitreal AAV8 exhibit poor transduction but showed no detectable intraocular inflammation.

Local inflammatory responses after suprachoroidal AAV8

We previously found that suprachoroidal AAV8 injection elicited greater local infiltration of inflammatory cells than transscleral subretinal or intravitreal injections at 1 month post-injection.[21] In this study, we further characterize the local inflammation using immunohistochemistry at 2 and 3 months after suprachoroidal AAV8 delivery (Figure 2). GFP transgene expression was detectable in both RPE and scleral tissues at 1 month, but only persisted in the sclera at months 2 and 3, appearing mostly in spindle-shaped cells that resemble scleral fibroblasts. The GFP expression in the sclera was not visible on live fundus imaging likely due to blockage of the fluorescence by the darkly-pigmented RPE and uvea in rhesus macaques.[33] Local infiltration of ionized calcium-binding adaptor-1 (Iba1)+ microglia and macrophages (Figures 2A-2E), CD45+ leukocytes (Figures 2F-2J), CD8+ cytotoxic T cells (Figures 2K-2O), as well as reactive gliosis as shown by glial fibrillary acidic protein (GFAP) staining (Figures 2P-2T), were detected through month 3 as compared to uninjected control animals. Interestingly, the outer retinal layers and RPE architecture appeared partly restored at month 3 in the animal that received systemic corticosteroids (Figures 2U-2Y). The animal that received low-dose suprachoroidal

AAV8 injections also demonstrated GFP expression in the sclera, and exhibited a similar degree of local inflammatory responses at month 3 (Figures 2D, 2I, 2N, 2S, 2X).

Humoral immune responses after suprachoroidal AAV8

To evaluate humoral immune response from B-cells, we employed a sandwich enzyme-linked immunosorbent assay (ELISA) to measure serum binding antibodies against the AAV8 capsid or GFP transgene product after suprachoroidal or intravitreal delivery of the AAV8 vector (Figures 3A and 3B). Most of the animals that received suprachoroidal AAV8 developed minimal antibody responses against the viral capsid, whereas the animal that received intravitreal AAV8 exhibited higher anti-AAV8 antibody levels within 1 month (Figure 3A). These results are consistent with our prior study which demonstrated higher concentrations of serum NAbs from intravitreal than suprachoroidal or subretinal AAV8 as measured using an *in vitro* transduction inhibition assay.[21] By contrast, only animals that received suprachoroidal AAV8 developed anti-GFP antibodies, which reached the highest levels at month 3, while the animal that received only intravitreal AAV8 did not (Figure 3B). As Rhesus 02 received high-dose suprachoroidal AAV8 in both eyes, we further validated the humoral response to GFP by performing flow cytometry on peripheral blood mononuclear cells (PBMCs) collected from the serum of this animal, and found expansion of GFP-responsive plasma B-cells (CD19-,CD27+,CD38+, HLADRlow) after suprachoroidal AAV8 injection (Figure 3C, Supplementary Figure 1) which likely accounts for the greater production of systemic anti-GFP antibodies. Interestingly, the animal that received low-dose AAV8 (Rhesus 01) developed similar concentrations of anti-GFP antibodies (Figure 3B). Together, these findings suggest that although intravitreal AAV8 produces an earlier and more robust humoral response to the viral capsid, suprachoroidal delivery triggers greater antibody

responses to GFP, possibly due to exposure of GFP-expressing scleral fibroblasts to systemic immune surveillance, given their location outside the blood-retinal barrier.

Cell-mediated immune responses after suprachoroidal AAV8

We next explored cell-mediated immune responses to suprachoroidal AAV8 using ELISpot assays to detect interferon-γ (IFN-γ)-producing T-cells against AAV8 or GFP in PBMCs collected throughout the study and in splenocytes collected at time of necropsy (Figure 4). None of the animals showed appreciable T-cell responses to the AAV8 capsid with the exception of Rhesus 01 which appeared to have pre-existing T-cell responses to AAV8 prior to injection (Figure 4A), despite not having anti-AAV8 antibodies (Figure 3A) or NAbs at baseline.[21] Similar to the humoral immune responses, suprachoroidal AAV8 also triggered T-cell responses to GFP beginning as early as 1 month after injection, particularly in animals that received suprachoroidal injections in both eyes (Figure 4B). Using splenocytes collected at necropsies, we found suprachoroidal AAV8 injection triggered greater T-cell responses to the GFP transgene product than to the viral vector (Figures 4C-4D, Supplementary Figure 2).

Systemic biodistribution of suprachoroidal AAV8

To evaluate systemic biodistribution after suprachoroidal AAV8 delivery, we performed quantitative PCR to detect the GFP transgene sequence in genomic DNA from peripheral organs including kidney, liver, and spleen. The highest genome copies were detected in the spleen, followed by the liver, and was undetectable in the kidney (Figure 5). Interestingly, the animal that received intravitreal injection of AAV8 in both eyes (Rhesus 05) showed much higher genome copies of the vector in the spleen and liver, as compared to animals that received suprachoroidal AAV8 in both eyes (Rhesus 01 and 02) or suprachoroidal and subretinal AAV8 in fellow eyes

(Rhesus 03 and 04). These studies suggest that suprachoroidal AAV delivery may result in some systemic distribution to peripheral organs such as the spleen and liver, but at much lower amounts than intravitreal injections.

Discussion

Despite the presence of ocular immune privilege, AAV-mediated gene delivery to the eye triggers host immune responses that may vary with AAV dose, serotype, route of delivery, and type of transgene. Early studies from the RPE65 gene therapy trials using an AAV2 vector reported a dose-dependent immune response with intraocular inflammation observed in the high-dose (1 x 10^{12} vg/eye), but not low-dose (1 x 10^{11} vg/eye) patient cohorts.[1] The presence of pre-existing immunity also varies with AAV serotypes, as seroprevalence of anti-AAV2 NAbs in humans has been reported to range between 30-60%, while NAbs against AAV7, AAV8, and AAV9 are lower at 15-30%.[34,35] Importantly, the route of vector delivery is a major determinant of host immune responses. Intravitreal injections of AAV2 and AAV8 triggers more intraocular inflammation, with more robust humoral and cellular immune responses in mice and NHPs than subretinal delivery,[13,16,36–38] presumably due to the greater egress of viral particles into systemic circulation from the vitreous cavity. In this study, we evaluated host immune responses to a novel mode of delivering viral vectors into the suprachoroidal space of NHPs using transscleral microneedles.[21,22] Using an AAV8 vector to express GFP under a CMV promoter, we found that suprachoroidal delivery can trigger a peripheral chorioretinitis and vitritis with outer retinal disruption at month 1 after viral injection, but subsequently showed resolution of inflammation and restoration of retinal architecture at month 3, after systemic corticosteroid administration. The inflammation was accompanied by both humoral and cell-mediated responses to the GFP transgene product, but a less pronounced humoral response to the AAV8 capsid than intravitreal injections.

The host immune responses to the GFP transgene and viral vector can be explained by the pattern of transgene expression, systemic biodistribution of the viral vectors, and unique location of the suprachoroidal space outside the blood-retinal barrier. The blood-retinal barrier is composed of an inner barrier that consists of retinal capillary endothelium, and an outer barrier formed by RPE tight junctions. While the vitreous cavity and subretinal space are immune-privileged ocular compartments within this barrier, the suprachoroidal space is adjacent to the highly-fenestrated choroidal vasculature and readily interfaces with macrophages in the choroid and sclera outside of this barrier. In contrast to intravitreal and subretinal injections which enabled focal GFP transduction within the neurosensory retina, suprachoroidal AAV8 produced broad regions of transgene expression in the RPE and sclera which are outside the blood-retinal barrier. RPE are potent antigen presenting cells (APCs) of the retina,[39,40] while macrophages and dendritic cells are prevalent in the sclera.[41] In our study, we observed Iba1+ macrophages/microglia surrounding GFP-expressing RPE, but did not clearly detect any GFP-expressing Iba1+ cells. While the exact cell type responsible for antigen presentation is unclear, our results suggest that immune sensitization likely occurs locally in the eye rather than in peripheral tissues, as both humoral and cellular immune responses to GFP appeared to correlate with the greater transgene expression in the sclera after suprachoroidal injections, regardless of AAV dose, rather than to the higher amounts of viral genomes in peripheral organs after intravitreal delivery. This hypothesis and our results are consistent with the study by Vanderberghe et al, in which T-cell responses against GFP but not AAV capsid were found in NHP eyes after subretinal AAV8 delivery.

Even though the suprachoroidal space is outside the blood-retinal barrier, intravitreal AAV8 triggered a more robust humoral response to the viral capsid, likely due to greater systemic exposure to the AAV8 vector as shown in our biodistribution studies. Trabecular outflow through

the canal of Schlemm accounts for 80-90% of vitreous and aqueous humor drainage from the eye, while uveoscleral outflow which likely mediates AAV egress from the suprachoroidal space is less efficient.[42] Our findings are consistent with previous studies demonstrating greater humoral immune responses after intravitreal versus subretinal injections,[36,37,43] and suggest that the suprachoroidal space may have better retention of viral particles than the vitreous cavity.

Although the current study focused on AAV8-binding antibodies, we previously found a similar pattern of NAb response that was also more pronounced after intravitreal than suprachoroidal AAV delivery. NAbs prevent viral particles from phagocytosis by blocking essential receptor interactions between the virus and host cells, and may also sequester AAV distribution to the spleen.[44] By contrast, the role of non-neutralizing antibodies is unclear, and may enhance the clearance of AAV vectors through opsonization or have the opposite effects of NAbs.[44,45] Interestingly, although serum NAbs can impact the re-administration of AAV given intravitreally,[43] they do not appear to affect the functional effectiveness of AAV readministered subretinally.[46] Because a major advantage of suprachoroidal AAV delivery is the capacity for repeated injections, future studies are necessary to determine if the effectiveness of suprachoroidal AAV re-administration may be impacted on repeated dosing.

Our biodistribution assays demonstrated greater peripheral distribution of viral genomes to the spleen and liver after intravitreal injections, compared with suprachoroidal AAV8 delivery, similar to findings by Seitz and colleagues who also found more viral genomes in peripheral organs after intravitreal versus subretinal AAV8 in NHPs.[47] The higher expression in the spleen alludes to a deviant immune response similar to anterior chamber associated immune deviation (ACAID) – a phenomenon in which immunogen bearing APCs from the eye migrate through the trabecular meshwork to the spleen, where afferent CD4+ Th1 cells and efferent CD8+ cytotoxic T cells

differentiate and mature.[15] Further studies to distinguish more pro-inflammatory from immunosuppressive T-cell subtypes could elucidate the nature of the host cellular immune responses, and help refine strategies for mitigation. The timing of T-cell-directed immunosuppression, for example, has been shown to impact transgene immunogenicity after subretinal AAV delivery.

There are several limitations to our study. Like humans, rhesus macaques are native hosts of AAVs without significant disease association,[48,49] but exhibit higher seroprevalence of pre-existing immunity to AAV8 capsids.[50,51] Although we pre-screened animals for the absence of NAbs against AAV8, one animal in our study was found to have a pre-existing T-cell response. Also, the AAV vectors in our study were not generated under Good Medical Practice (GMP) conditions, and may exhibit greater immunogenicity. In addition, although NHPs are excellent preclinical models due to their similar ocular anatomy and immune responses, they do not mount the same level of AAV-specific T-cell responses as humans in liver-directed gene transfer, possibly due to differences in AAV life cycles between humans and NHPs, more efficient recruitment of primed human T-cells to the liver,[52–54] or loss of inhibitory sialic acid-recognizing Ig superfamily lectins on human T-cells. Finally, because two animals in our study also had subretinal AAV injections in their contralateral eyes, their immune responses may not fully reflect the consequences of suprachoroidal delivery. However, as previous studies have shown that subretinal injections elicit minimal humoral or cellular responses,[13,37] we believe that the immune responses in these animals are more likely attributable to the suprachoroidal injections.

Suprachoroidal injection of AAV8 is currently under evaluation in human clinical trials for expressing a monoclonal antibody fragment to neutralize vascular endothelial growth factor for treatment of neovascular age-related macular degeneration. Unlike the GFP transgene in our study

which is a known immunogen and not native to primate species,[55] these ongoing human trials employ human-based transgenes and are less likely to generate as robust an immune response. Our study also employed a CMV promoter which has been associated with ocular toxicity not otherwise observed using photoreceptor-specific promoters for AAV transgene expression.[56] Future studies that employ human-derived and more clinically-relevant promoters and transgenes could better predict host immune responses after suprachoroidal AAV injections, and help facilitate clinical translation of this unique route of vector delivery for retinal gene therapy.

Materials and Methods

Animals

The California National Primate Research Center (CNPRC) is accredited by the Association for Assessment and Accreditation of Laboratory Animal Care (AAALAC) International. All studies using rhesus macaques (*Macaca mulatta*) followed the guidelines of the Association for Research in Vision and Ophthalmology (ARVO) Statement for the Use of Animals in Ophthalmic and Vision Research, and complied with the National Institutes of Health (NIH) Guide for the Care and Use of Laboratory Animals. All procedures were conducted under protocols approved by the University of California, Davis Institutional Animal Care and Use Committee (IACUC).

AAV8 production and intraocular injection

The AAV cis construct which expresses enhanced GFP under a CMV promoter was packaged into AAV8 capsid and purified by the UC Davis NEI Vision Molecular Construct and Packaging Core. After animal sedation, eyes were sterilely prepped with 1% povidone-iodine and flushed with sterile saline, followed by placement of an eyelid speculum. For transcleral microneedle injections, a 700 μm-long 30-gauge microneedle (Clearside Biomedical) was inserted through the conjunctiva and sclera at 4 mm or 10 mm posterior to the corneal limbus to inject into in the superotemporal quadrant (single 100 μL injection) of left eyes, and both superotemporal and inferonasal quadrants (two 50 μL injections) of right eyes. For intravitreal injections, a 0.5 inch-long 30-gauge needle (BD biosciences) was inserted through the pars plana, 4 mm posterior to the limbus, in the inferotemporal quadrant (single 100 μL injection) of both eyes. The viral concentrations are reported in Supplementary Figure 1. Intraocular pressure (IOP) was measured

following intraocular injections, and an anterior chamber tap was performed using a 30-gauge needle to remove aqueous until the IOP was normalized.

Rhesus 02 which received high-dose suprachoroidal AAV8 showed signs of ocular irritation and was found to have mild AC cells at 2 weeks after the injection, and was treated with oral prednisone (1mg/kg) for 2 weeks. In Rhesus 03, 04, and 05, a 40 mg periorbital subtenon injection of triamcinolone acetonide suspension (Kenalog-40, Bristol-Myers-Squibb) was also given in the superotemporal quadrant at the request of the veterinarian to prevent uveitis.

Imaging

All animals underwent SLO and SD-OCT imaging using the Spectralis HRA+OCT device (Heidelberg Engineering, Heidelberg, Germany) before and at 1 week, 1 month, and 2 or 3 months after AAV injections. Confocal SLO was used to capture 55° x 55° or 30º x 30º fluorescence images using 488 nm excitation light and a long-pass barrier filter starting at 500 nm. Images were captured from the central macula and from the peripheral retina by manually steering the Spectralis device. Due to the facial contour of these animals, the superior quadrants could be seen on live visualization but was difficult to capture at sufficient quality for image montage. SD-OCT was performed alongside infrared reflectance images using an 820 nm diode laser to capture 30 º x 5º SD-OCT raster scans with 1536 A-scans per B-scan and 234 μm spacing between B-scans, in high-resolution mode. SD-OCT scans were captured from the central macula and in regions of visible GFP fluorescence, especially near the junction between transduced and untransduced tissues. 25 scans were averaged for each B-scan, using the Heidelberg eye tracking Automatic Real-Time (ART) software. Animals also underwent color fundus photography (CF-1, Canon) for documentation of clinical exam findings when possible.

PBMC and splenocyte collection

For PBMC isolation, anticoagulated blood was diluted in phosphate buffered saline (PBS), layered over Ficoll Paque Premium (GE Healthcare, 17544202), and centrifuged for 30 minutes at 800 x g. The PBMC fraction was transferred to PBS and centrifuged again, followed by lysis of red blood cells using Ammonium-Chloride-Potassium (ACK) lysis buffer (Gibco, A1049201), washing with Roswell Park Memorial Institute (RPMI) buffer, and resuspension in 10% dimethyl sulfoxide (DMSO) in heat-inactivated fetal bovine saline (FBS). For splenocyte collection, spleen tissues were homogenized in sterile PBS, passed through a cell strainer, centrifuged, then resuspended in ACK lysis buffer, washed with PBS, and resuspended in 10% DMSO in FBS.

Binding antibody assay

Binding antibody assays were performed to detect antibodies against GFP and AAV capsid in NHP sera as described previously.[38] For anti-AAV8 antibody detection, a sandwich-ELISA kit designed for AAV8 titration was used (Progen, PRAAV8). Briefly, microtiter strips with AAV8-specific antibodies were incubated with AAV8 particles ($2x10^{12}$ vg/mL) overnight at 4°C, blocked with 5% milk in PBS, then incubated with macaque sera (1:1000 dilution) at 37°C for 2 hours. After washing, the strips were incubated with horse radish peroxidase (HRP)-conjugated anti-rhesus secondary antibodies (Southern biotech, 6200-50, 1:2000) for 2 additional hours at room temperature, incubated with 3,3',5,5'-tetramethylbenzidine (TMB; Southern Biotech, 0410-01), stopped with a stopping solution (Southern Biotech, 0412-01), then read with a plate reader (Fisher Scientific accuSkan FC, N16612) with 450 nm absorbance. For detecting anti-GFP antibodies, a 96-well plate was coated with enhanced GFP protein (BioVision, 4999-100, 5 µg/mL) overnight at 4°C, blocked with 5% non-fat milk in PBS, then incubated with diluted serum samples (1:5000) at 37°C for 2 hours followed by detection with HRP-conjugated anti-rhesus IgG as described above. Commercial anti-AAV8 (Progen, 610160S, 1:100) and anti-GFP (Abcam, ab6556, 1:1000)

antibodies were used as positive controls, and all values were determined from triplicates. The antibodies were calculated against a standard curve and normalized with total protein.

Enzyme-linked immune absorbent spot (ELISpot)

ELISpot assays to detect IFN-γ-secreting cells from PBMCs were performed with a commercial kit according to the manufacturer's instruction (U-CyTech, CT121). Briefly, a 96-well PVDF membrane-bottomed plate was activated with 70% ethanol, and coated with anti-IFN-γ antibodies overnight at 4°C. After washing and blocking, PBMCs were seeded at $4x10^5$ cells per well in RPMI-160 media containing a mix of 182 AAV8 capsid or enhanced GFP peptides (15mers and 11 overlaps, 4 ng/uL, JPT, PM-AAV8-CP, PM-EGFP) for 48 hours. We incubated the cells with Phorbol 12-myristate 13-acetate (PMA, 80 nM) and ionomycin (1.3 μM) for positive control, and DMSO (0.05%) for negative control. After removing the cells, the plate was incubated with biotinylated detection antibody for 2 hours followed by Stretavidin-HRP and 3-Amino-9-ethylcarbazole (AEC) substrate. Spots were counted and normalized with negative control. Spot forming unit (SFU) was calculated from triplicates converted to SFU per 10^6 cells.

Quantitative polymerase chain reaction

Systemic biodistribution assays were performed using qPCR with SYBR Green. Liver, spleen and kidney samples were collected at necropsy, and genomic DNA (gDNA) extracted using a commercial kit following the manufacturer's instruction (Qiagen, 69504). For qPCR, each reaction contained 10 ng of gDNA with SYBR green qPCR master mix (Invitrogen) and forward and reverse primers. qPCR cycling was 95°for 10 min, and 40 cycles of 95°for 10 min, 60°for 1 min, and melting curve analysis was performed for primer dimers. Copy number of GFP transgene was calculated against standard curve, and rhesus beta actin primer set was used as an internal

control in a separate reaction. The primer sets used in this study are enhanced GFP forward 5'-AGATCCGCCACAACATCGAGG-3', GFP reverse 5'-AGCAGGACCATGTGATCGC-3', beta-actin forward 5'-GGGCCGGACTCGTCATAC-3' and beta-actin reverse 5'-CCTGGCACCCAGCACAAT-3'. The limit of detection was 162 copies/µg DNA.

Immunohistochemistry

Immunohistochemistry was performed as described previously.[21] Posterior eye cups were fixed with 4% paraformaldehyde (PFA) for 2 hours after removal of anterior segments lens and vitreous. After washing with PBS, tissues were cryoprotected with 30% sucrose overnight, then embedded and cryosectioned at 18µm. For antibody labelling, sections were washed with PBS, blocked with 10% normal donkey serum for 30 min, then incubated in primary antibody for 1-2 hours at room temperature, followed by Alexa Fluor-conjugated secondary antibodies. Primary antibodies include IBA-1 (Wako, AB10558, 1:100), GFAP (Dako, Z0334, 1:200), and CD45 (BD, 552566, 2.5µg/ml).

Flowcytometry

For flow cytometry, 0.5 x 10^6 PBMCs or splenocytes per well were plated in duplicate in 96-well plates in RPMI supplemented with 10% FBS for 24 hours. The cells were stimulated with AAV8 peptide (4ng/µl, JPT, PM-AAV8-CP), GFP peptide (4ng/µl, JPT, PM-EGFP), cRPMI alone (unstimulated), or with PMA (80 nM)-Ionomycin(1.3 µM) (positive control). Cultures were incubated at 37°C for 48 hours, washed with PBS, and stained for flow cytometric analysis. The cells were incubated with 50µL of an antibody cocktail for CD8 (Thermo Fisher, Q10055), HLADR (BioLegend, 307656), CD19 (BioLegend, 302239), CD27 (Biolegend, 302824), and CD38 (Labcome, 100825) for 30 minutes at room temperature in the dark, followed by 2 washes

418 with FACS buffer (PBS + 1% FBS), and resuspended in 300 µL of FACS buffer for analysis. The
419 data were acquired within an hour on a BD FACS LSR II flow cytometer (Beckman Coulter Life
420 Sciences, USA).

421

Acknowledgements

We thank Marie Burns and Huaiyang Chen for AAV production, Amanda Carpenter for PBMC and splenocyte preparation, Jeffrey Roberts and John Morrison for CNPRC logistics, Monica Motta for assistance with animal imaging, and Dennis Hartigan-O'Connor for discussions. We also thank Clearside Biomedical and Glenn Noronha, Jesse Yoo, and Donna Taraborelli for providing the suprachoroidal microneedles used in our study. This study was supported by the California National Primate Research Center pilot grant program and base grant NIH P510D011107. GY is supported by NIH K08 EY026101, NIH R21 EY031108, and Macula Society. ST is supported by U24 U24EY029904. The AAV8 vector was produced by the Center for Vision Sciences Molecular Constructs and Packaging core facility supported by NIH P30 EY012576. No funding organizations had any role in the design or conduct of this research. The content is solely the responsibility of the authors and does not necessarily represent the official views of the funding agencies.

Author Contributions

G.Y conceived the study design, obtained funding, performed the examinations, intraocular injections, and in vivo imaging, and supervised the study. S.H.C, T.S, and T.N conducted the binding antibody assays, ELIspot assays, biodistribution studies, and immunohistochemistry. I.M assisted clinical examination, injections, and tissue collection. A.M conducted flow cytometry and analyzed data. G.Y and S.H.C analyzed all data and wrote the manuscript. G.Y, S.H.C, T.C, P.S and S.T critically reviewed the manuscript.

Disclosures / Conflicts of Interest: G.Y. received research support from Clearside Biomedical, Genentech, and Iridex, and personal fees for consultancy from Alimera, Allergan, Carl Zeiss

444 Meditec, Clearside Biomedical, Genentech, Iridex, Topcon, and Verily. T.C is an employee with
445 and has equity ownership in Clearside Biomedical. Transscleral microneedles used in this study
446 were provided by Clearside Biomedical, and may be requested under Material Transfer Agreement
447 (MTA).

448

449 References

450 1. Bainbridge JWB, Mehat MS, Sundaram V, et al. Long-Term Effect of Gene Therapy on
451 Leber's Congenital Amaurosis. *New England Journal of Medicine*. 2015;372(20):1887-1897.
452 doi:10.1056/NEJMoa1414221

453 2. Bainbridge JWB, Smith AJ, Barker SS, et al. Effect of Gene Therapy on Visual Function in
454 Leber's Congenital Amaurosis. *New England Journal of Medicine*. 2008;358(21):2231-2239.
455 doi:10.1056/NEJMoa0802268

456 3. Maguire AM, Simonelli F, Pierce EA, et al. Safety and Efficacy of Gene Transfer for
457 Leber's Congenital Amaurosis. *New England Journal of Medicine*. 2008;358(21):2240-2248.
458 doi:10.1056/NEJMoa0802315

459 4. Maguire AM, High KA, Auricchio A, et al. Age-dependent effects of RPE65 gene therapy
460 for Leber's congenital amaurosis: a phase 1 dose-escalation trial. *Lancet*.
461 2009;374(9701):1597-1605. doi:10.1016/S0140-6736(09)61836-5

462 5. Cideciyan AV, Hauswirth WW, Aleman TS, et al. Vision 1 Year after Gene Therapy for
463 Leber's Congenital Amaurosis. *N Engl J Med*. 2009;361(7):725-727.
464 doi:10.1056/NEJMc0903652

465 6. Hauswirth WW, Aleman TS, Kaushal S, et al. Treatment of Leber Congenital Amaurosis
466 Due to RPE65 Mutations by Ocular Subretinal Injection of Adeno-Associated Virus Gene
467 Vector: Short-Term Results of a Phase I Trial. *Hum Gene Ther*. 2008;19(10):979-990.
468 doi:10.1089/hum.2008.107

7. Wang D, Tai PWL, Gao G. Adeno-associated virus vector as a platform for gene therapy delivery. *Nat Rev Drug Discov*. 2019;18(5):358-378. doi:10.1038/s41573-019-0012-9

8. Manno CS, Pierce GF, Arruda VR, et al. Successful transduction of liver in hemophilia by AAV-Factor IX and limitations imposed by the host immune response. *Nat Med*. 2006;12(3):342-347. doi:10.1038/nm1358

9. Wang Z, Allen JM, Riddell SR, et al. Immunity to adeno-associated virus-mediated gene transfer in a random-bred canine model of Duchenne muscular dystrophy. *Hum Gene Ther*. 2007;18(1):18-26. doi:10.1089/hum.2006.093

10. Halbert CL, Standaert TA, Aitken ML, Alexander IE, Russell DW, Miller AD. Transduction by adeno-associated virus vectors in the rabbit airway: efficiency, persistence, and readministration. *J Virol*. 1997;71(8):5932-5941. Accessed September 14, 2020. https://www.ncbi.nlm.nih.gov/pmc/articles/PMC191849/

11. Kessler PD, Podsakoff GM, Chen X, et al. Gene delivery to skeletal muscle results in sustained expression and systemic delivery of a therapeutic protein. *Proc Natl Acad Sci U S A*. 1996;93(24):14082-14087. Accessed September 14, 2020. https://www.ncbi.nlm.nih.gov/pmc/articles/PMC19498/

12. Xiao W, Chirmule N, Schnell MA, Tazelaar J, Hughes JV, Wilson JM. Route of Administration Determines Induction of T-Cell-Independent Humoral Responses to Adeno-Associated Virus Vectors. *Molecular Therapy*. 2000;1(4):323-329. doi:10.1006/mthe.2000.0045

13. Li Q, Miller R, Han P-Y, et al. Intraocular route of AAV2 vector administration defines humoral immune response and therapeutic potential. *Mol Vis*. 2008;14:1760-1769.

14. Shirley JL, Jong YP de, Terhorst C, Herzog RW. Immune Responses to Viral Gene Therapy Vectors. *Molecular Therapy*. 2020;28(3):709-722. doi:10.1016/j.ymthe.2020.01.001

15. Streilein JW. Ocular immune privilege: therapeutic opportunities from an experiment of nature. *Nat Rev Immunol*. 2003;3(11):879-889. doi:10.1038/nri1224

16. Barker SE, Broderick CA, Robbie SJ, et al. Subretinal delivery of adeno-associated virus serotype 2 results in minimal immune responses that allow repeat vector administration in immunocompetent mice. *J Gene Med*. 2009;11(6):486-497. doi:10.1002/jgm.1327

17. Bennett J, Ashtari M, Wellman J, et al. AAV2 Gene Therapy Readministration in Three Adults with Congenital Blindness. *Sci Transl Med*. 2012;4(120):120ra15. doi:10.1126/scitranslmed.3002865

18. Dalkara D, Byrne LC, Klimczak RR, et al. In Vivo–Directed Evolution of a New Adeno-Associated Virus for Therapeutic Outer Retinal Gene Delivery from the Vitreous. *Science Translational Medicine*. 2013;5(189):189ra76-189ra76. doi:10.1126/scitranslmed.3005708

19. Petrs-Silva H, Dinculescu A, Li Q, et al. Novel Properties of Tyrosine-mutant AAV2 Vectors in the Mouse Retina. *Mol Ther*. 2011;19(2):293-301. doi:10.1038/mt.2010.234

20. Lukason M, DuFresne E, Rubin H, et al. Inhibition of Choroidal Neovascularization in a Nonhuman Primate Model by Intravitreal Administration of an AAV2 Vector Expressing a Novel Anti-VEGF Molecule. *Mol Ther*. 2011;19(2):260-265. doi:10.1038/mt.2010.230

21. Yiu G, Chung SH, Mollhoff IN, et al. Suprachoroidal and Subretinal Injections of AAV Using Transscleral Microneedles for Retinal Gene Delivery in Nonhuman Primates. *Molecular Therapy - Methods & Clinical Development*. 2020;16:179-191. doi:10.1016/j.omtm.2020.01.002

22. Ding K, Shen J, Hafiz Z, et al. AAV8-vectored suprachoroidal gene transfer produces widespread ocular transgene expression. *J Clin Invest*. 2019;129(11):4901-4911. doi:10.1172/JCI129085

23. Yiu G, Pecen P, Sarin N, et al. Characterization of the Choroid-Scleral Junction and Suprachoroidal Layer in Healthy Individuals on Enhanced-Depth Imaging Optical Coherence Tomography. *JAMA Ophthalmol*. 2014;132(2):174-181. doi:10.1001/jamaophthalmol.2013.7288

24. Emami-Naeini P, Yiu G. Medical and Surgical Applications for the Suprachoroidal Space. *Int Ophthalmol Clin*. 2019;59(1):195-207. doi:10.1097/IIO.0000000000000251

25. Willoughby AS, Vuong VS, Cunefare D, et al. Choroidal Changes after Suprachoroidal Injection of Triamcinolone in Eyes with Macular Edema Secondary to Retinal Vein Occlusion. *Am J Ophthalmol*. 2018;186:144-151. doi:10.1016/j.ajo.2017.11.020

26. Lampen SIR, Khurana RN, Noronha G, Brown DM, Wykoff CC. Suprachoroidal Space Alterations Following Delivery of Triamcinolone Acetonide: Post-Hoc Analysis of the Phase 1/2 HULK Study of Patients With Diabetic Macular Edema. *Ophthalmic Surg Lasers Imaging Retina*. 2018;49(9):692-697. doi:10.3928/23258160-20180831-07

27. Kim YC, Edelhauser HF, Prausnitz MR. Targeted Delivery of Antiglaucoma Drugs to the Supraciliary Space Using Microneedles. *Invest Ophthalmol Vis Sci*. 2014;55(11):7387-7397. doi:10.1167/iovs.14-14651

28. Olsen TW, Feng X, Wabner K, et al. Cannulation of the Suprachoroidal Space: A Novel Drug Delivery Methodology to the Posterior Segment. *American Journal of Ophthalmology*. 2006;142(5):777-787.e2. doi:10.1016/j.ajo.2006.05.045

29. Olsen TW, Feng X, Wabner K, Csaky K, Pambuccian S, Cameron JD. Pharmacokinetics of Pars Plana Intravitreal Injections versus Microcannula Suprachoroidal Injections of Bevacizumab in a Porcine Model. *Invest Ophthalmol Vis Sci*. 2011;52(7):4749-4756. doi:10.1167/iovs.10-6291

30. Patel SR, Berezovsky DE, McCarey BE, Zarnitsyn V, Edelhauser HF, Prausnitz MR. Targeted Administration into the Suprachoroidal Space Using a Microneedle for Drug Delivery to the Posterior Segment of the Eye. *Invest Ophthalmol Vis Sci*. 2012;53(8):4433-4441. doi:10.1167/iovs.12-9872

31. Patel SR, Lin ASP, Edelhauser HF, Prausnitz MR. Suprachoroidal Drug Delivery to the Back of the Eye Using Hollow Microneedles. *Pharm Res*. 2011;28(1):166-176. doi:10.1007/s11095-010-0271-y

32. Yeh S, Khurana RN, Shah M, et al. Efficacy and Safety of Suprachoroidal CLS-TA for Macular Edema Secondary to Noninfectious Uveitis: Phase 3 Randomized Trial. *Ophthalmology*. 2020;127(7):948-955. doi:10.1016/j.ophtha.2020.01.006

549 33. Yiu G, Vuong VS, Oltjen S, et al. Effect of Uveal Melanocytes on Choroidal Morphology in
550 Rhesus Macaques and Humans on Enhanced-Depth Imaging Optical Coherence
551 Tomography. *Invest Ophthalmol Vis Sci*. 2016;57(13):5764. doi:10.1167/iovs.16-20070

552 34. Vandamme C, Adjali O, Mingozzi F. Unraveling the Complex Story of Immune Responses
553 to AAV Vectors Trial After Trial. *Hum Gene Ther*. 2017;28(11):1061-1074.
554 doi:10.1089/hum.2017.150

555 35. Calcedo R, Vandenberghe LH, Gao G, Lin J, Wilson JM. Worldwide Epidemiology of
556 Neutralizing Antibodies to Adeno-Associated Viruses. *J Infect Dis*. 2009;199(3):381-390.
557 doi:10.1086/595830

558 36. MacLachlan TK, Lukason M, Collins M, et al. Preclinical Safety Evaluation of AAV2-
559 sFLT01— A Gene Therapy for Age-related Macular Degeneration. *Mol Ther*.
560 2011;19(2):326-334. doi:10.1038/mt.2010.258

561 37. Reichel FF, Peters T, Wilhelm B, et al. Humoral Immune Response After Intravitreal But
562 Not After Subretinal AAV8 in Primates and Patients. *Invest Ophthalmol Vis Sci*.
563 2018;59(5):1910-1915. doi:10.1167/iovs.17-22494

564 38. Reichel FF, Dauletbekov DL, Klein R, et al. AAV8 Can Induce Innate and Adaptive Immune
565 Response in the Primate Eye. *Mol Ther*. 2017;25(12):2648-2660.
566 doi:10.1016/j.ymthe.2017.08.018

567 39. Osusky R, Dorio RJ, Arora YK, Ryan SJ, Walker SM. MHC class II positive retinal pigment
568 epithelial (RPE) cells can function as antigen-presenting cells for microbial superantigen.
569 *Ocul Immunol Inflamm*. 1997;5(1):43-50. doi:10.3109/09273949709085049

40. Lipski DA, Dewispelaere R, Foucart V, et al. MHC class II expression and potential antigen-presenting cells in the retina during experimental autoimmune uveitis. *J Neuroinflammation*. 2017;14(1):136. doi:10.1186/s12974-017-0915-5

41. Schlereth SL, Kremers S, Schrödl F, Cursiefen C, Heindl LM. Characterization of Antigen-Presenting Macrophages and Dendritic Cells in the Healthy Human Sclera. *Invest Ophthalmol Vis Sci*. 2016;57(11):4878-4885. doi:10.1167/iovs.15-18552

42. Karpinich NO, Caron KM. Schlemm's canal: more than meets the eye, lymphatics in disguise. *J Clin Invest*. 2014;124(9):3701-3703. doi:10.1172/JCI77507

43. Kotterman MA, Yin L, Strazzeri JM, Flannery JG, Merigan WH, Schaffer DV. Antibody neutralization poses a barrier to intravitreal adeno-associated viral vector gene delivery to non-human primates. *Gene Ther*. 2015;22(2):116-126. doi:10.1038/gt.2014.115

44. Wang L, Calcedo R, Bell P, et al. Impact of pre-existing immunity on gene transfer to nonhuman primate liver with adeno-associated virus 8 vectors. *Hum Gene Ther*. 2011;22(11):1389-1401. doi:10.1089/hum.2011.031

45. Fitzpatrick Z, Leborgne C, Barbon E, et al. Influence of Pre-existing Anti-capsid Neutralizing and Binding Antibodies on AAV Vector Transduction. *Mol Ther Methods Clin Dev*. 2018;9:119-129. doi:10.1016/j.omtm.2018.02.003

46. Amado D, Mingozzi F, Hui D, et al. Safety and efficacy of subretinal readministration of a viral vector in large animals to treat congenital blindness. *Sci Transl Med*. 2010;2(21):21ra16. doi:10.1126/scitranslmed.3000659

590 47. Seitz IP, Michalakis S, Wilhelm B, et al. Superior Retinal Gene Transfer and Biodistribution
591 Profile of Subretinal Versus Intravitreal Delivery of AAV8 in Nonhuman Primates. *Invest*
592 *Ophthalmol Vis Sci*. 2017;58(13):5792. doi:10.1167/iovs.17-22473

593 48. Calcedo R, Wilson JM. Humoral Immune Response to AAV. *Front Immunol*. 2013;4.
594 doi:10.3389/fimmu.2013.00341

595 49. Boutin S, Monteilhet V, Veron P, et al. Prevalence of serum IgG and neutralizing factors
596 against adeno-associated virus (AAV) types 1, 2, 5, 6, 8, and 9 in the healthy population:
597 implications for gene therapy using AAV vectors. *Hum Gene Ther*. 2010;21(6):704-712.
598 doi:10.1089/hum.2009.182

599 50. Gao G, Alvira MR, Somanathan S, et al. Adeno-associated viruses undergo substantial
600 evolution in primates during natural infections. *Proc Natl Acad Sci USA*.
601 2003;100(10):6081-6086. doi:10.1073/pnas.0937739100

602 51. Calcedo R, Morizono H, Wang L, et al. Adeno-associated virus antibody profiles in
603 newborns, children, and adolescents. *Clin Vaccine Immunol*. 2011;18(9):1586-1588.
604 doi:10.1128/CVI.05107-11

605 52. Guidotti LG, Iannacone M. Effector CD8 T cell trafficking within the liver. *Mol Immunol*.
606 2013;55(1):94-99. doi:10.1016/j.molimm.2012.10.032

607 53. Lang KS, Georgiev P, Recher M, et al. Immunoprivileged status of the liver is controlled by
608 Toll-like receptor 3 signaling. *J Clin Invest*. 2006;116(9):2456-2463. doi:10.1172/JCI28349

609 54. Nguyen DH, Hurtado-Ziola N, Gagneux P, Varki A. Loss of Siglec expression on T
610 lymphocytes during human evolution. *Proc Natl Acad Sci USA*. 2006;103(20):7765-7770.
611 doi:10.1073/pnas.0510484103

612 55. Ansari AM, Ahmed AK, Matsangos AE, et al. Cellular GFP Toxicity and Immunogenicity:
613 Potential Confounders in in Vivo Cell Tracking Experiments. *Stem Cell Rev Rep*.
614 2016;12(5):553-559. doi:10.1007/s12015-016-9670-8

615 56. Huang X, Zhou G, Wu W, et al. Genome editing abrogates angiogenesis in vivo. *Nature*
616 *Communications*. 2017;8(1):112. doi:10.1038/s41467-017-00140-3

617

618

Figures

Figure 1.

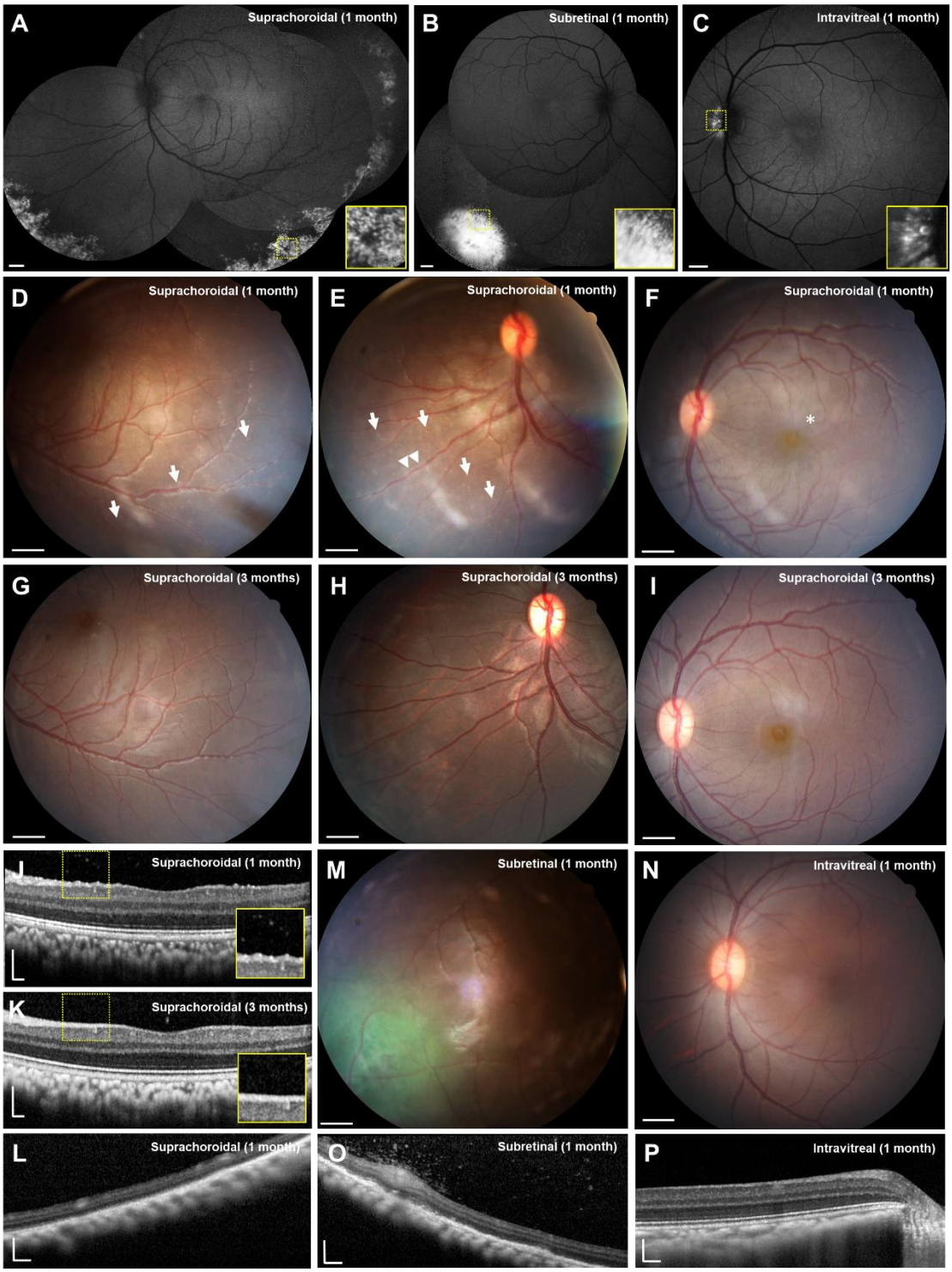

622 Figure 2.

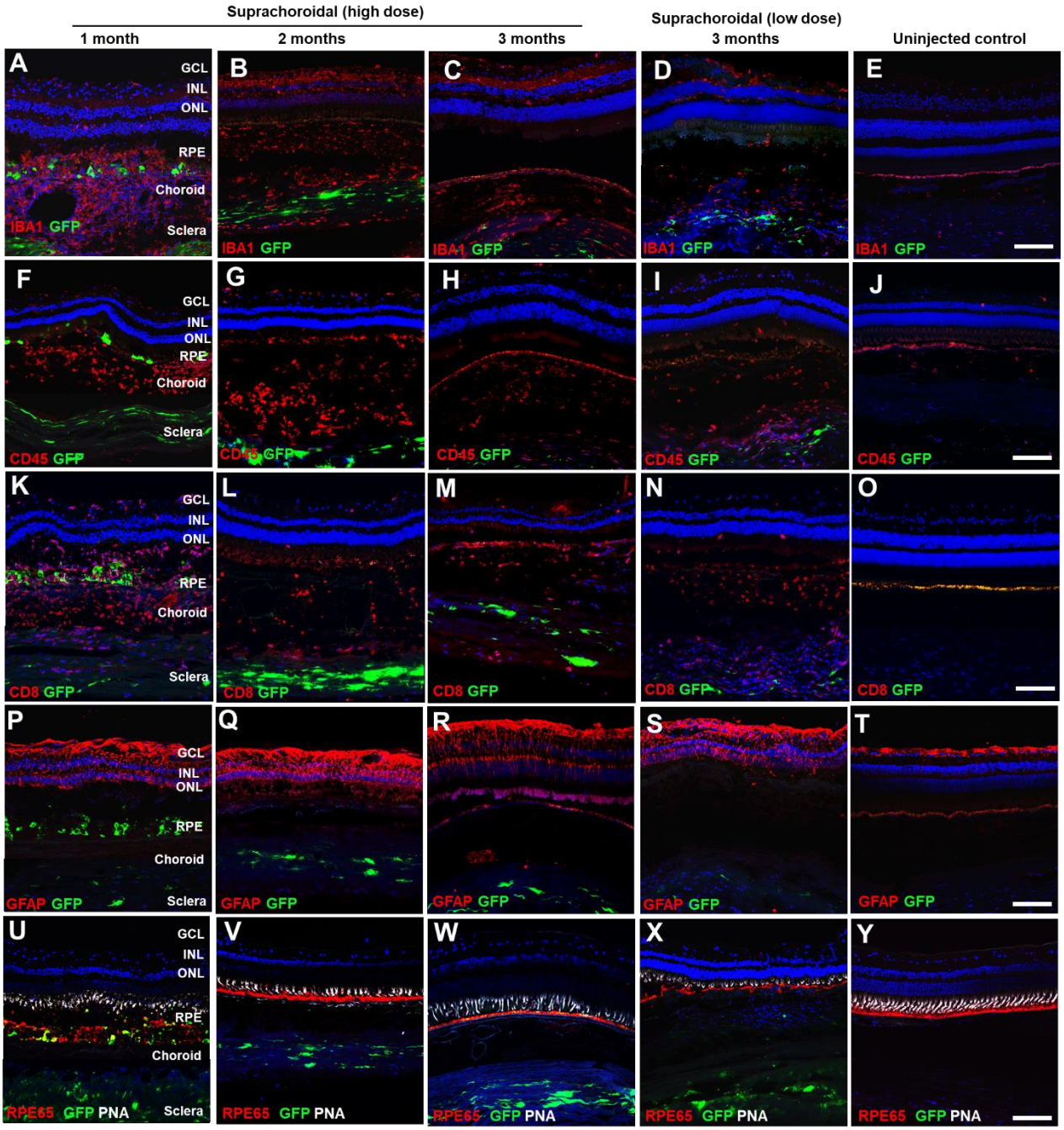

623

624

625 Figure 3.

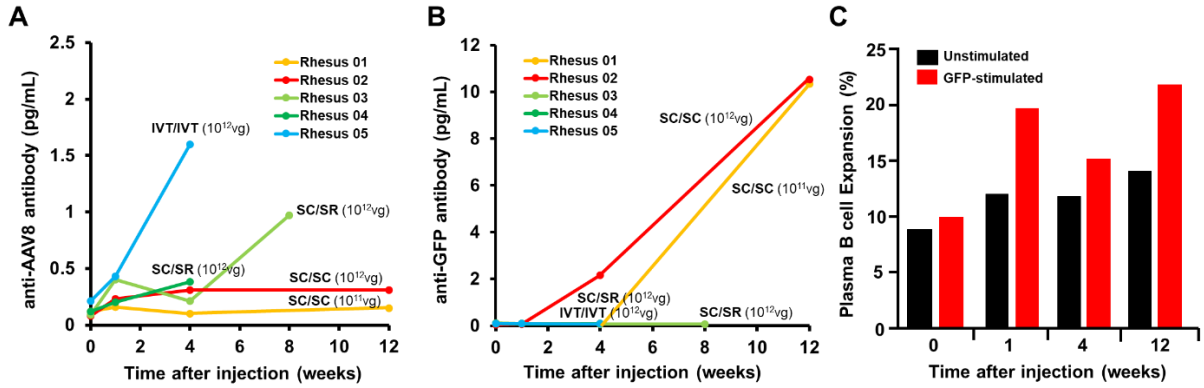

626

627

628

629 Figure 4.

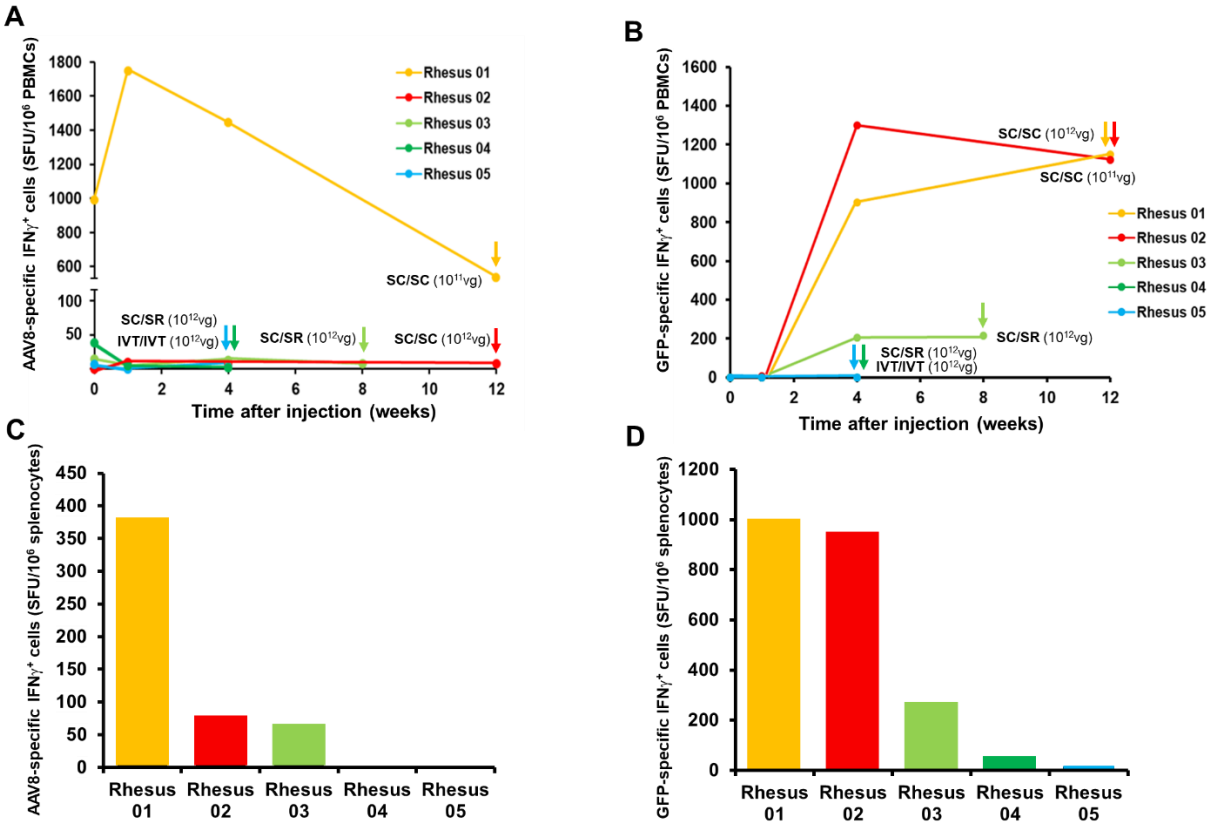

630

631

632 Figure 5.

633

634

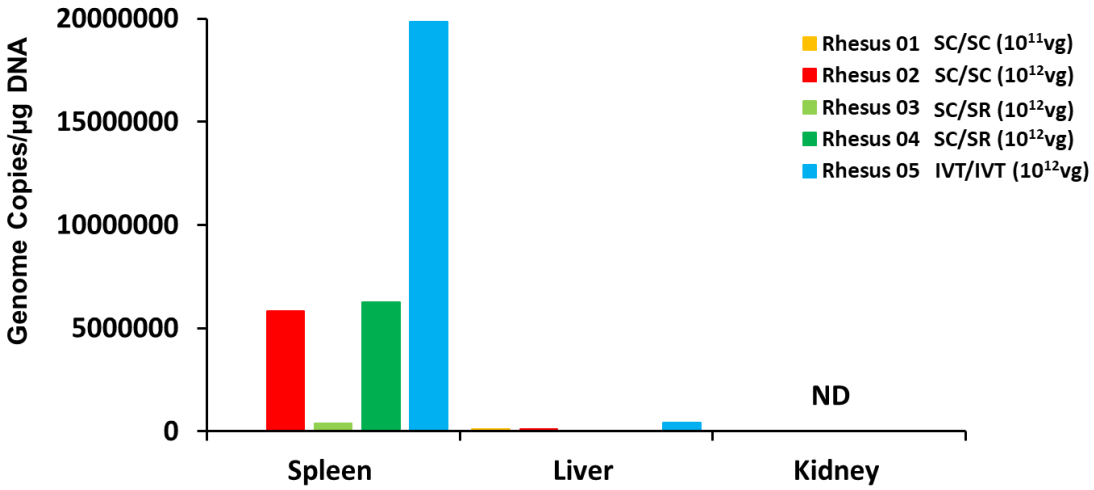

635

636

637 Supplementary Table 1

Animal ID	Age (Years)	Sex	Injection Mode (OD/OS)	Viral Dose (vg/eye)	Necropsy Date
Rhesus 01	10.25	Female	SC/SC	$7x10^{11}$ vg	Month 3
Rhesus 02	9.05	Female	SC/SC	$7x10^{12}$ vg	Month 3
Rhesus 03	5.47	Male	SR/SC	$7x10^{12}$ vg	Month 2
Rhesus 04	9.38	Female	SR/SC	$7x10^{12}$ vg	Month 1
Rhesus 05	10.38	Male	IVT/IVT	$7x10^{12}$ vg	Month 1

638

639 Abbreviations: OD, right eye; OS, left eye; IVT, intravitreal; SC, suprachoroidal; SR, subretinal; vg, viral genome

640 Supplementary Figure 1

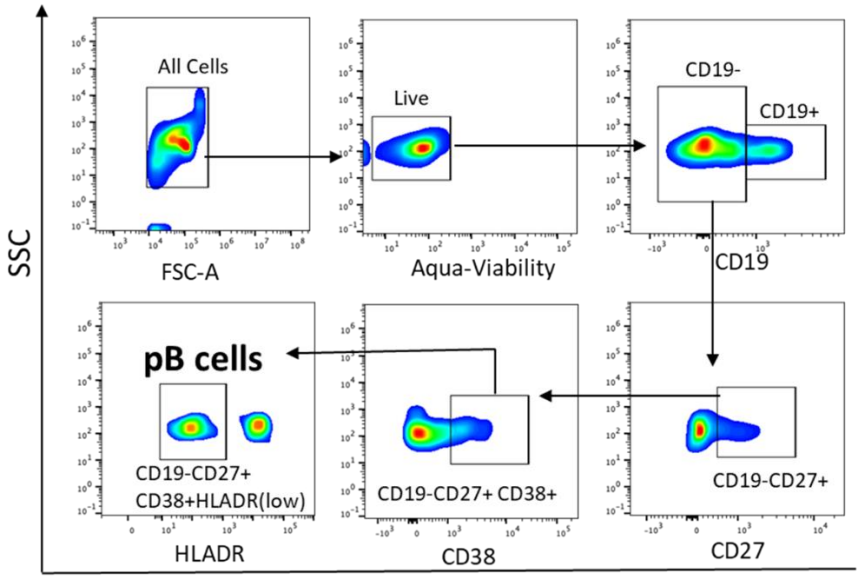

641

642

643 **Figure Legends**

644 **[Figure 1]** Multimodal ocular imaging after suprachoroidal, subretinal, or intravitreal injections
645 of AAV8 to express enhanced GFP in NHP eyes. **(A-C)** Representative scanning laser
646 ophthalmoscopy (SLO) montages and magnified insets of the yellow-dashed regions show
647 different patterns of GFP transgene expression at 1 month after suprachoroidal (A), subretinal (B),
648 and intravitreal (C) AAV delivery. **(D-I)** Representative color fundus photographs demonstrate
649 punctate spots (arrows), perivascular sheathing (arrowheads), and radial macular striae (asterisk)
650 that are observed after suprachoroidal AAV8 injections at 1 month (D-F), but resolved by 3 months
651 (G-I), consistent with a transient chorioretinitis and vasculitis. **(J-L)** Representative spectral-
652 domain optical coherence tomography (SD-OCT) images and magnified insets of the yellow-
653 dashed regions reveal hyperreflective foci seen after suprachoroidal AAV8 at 1 month (J) but not
654 at 3 months (K) or in peripheral retina (L). **(M-N)** Fundus photographs of macaque eyes
655 demonstrate GFP fluorescence after subretinal AAV8 (M), and no clear inflammation after
656 subretinal or intravitreal AAV8 (N). **(O-P)** SD-OCT images showed that subretinal AAV8 also
657 induced cellular extravasation from retinal vessels suggestive of a localized vasculitis (O), but not
658 after intravitreal injections (P). Scale bars, 1 mm for SLO images and fundus photos; 200 μm for
659 SD-OCT images.

660

661 **[Figure 2]** Local immune cell infiltration after suprachoroidal delivery of AAV8 in NHP eyes. **(A-**
662 **Y)** Confocal fluorescence images of GFP transgene expression (green) co-immunostained with
663 antibodies to IBA-1+ microglial cells (A-E), CD45+ leukocytes (F-J), CD8+ cytotoxic T-cells (K-
664 O), and GFAP+ reactive gliosis (P-T), as well as RPE65 (red) to label RPE cells and peanut
665 agglutinin (PNA, white) to label cone photoreceptor inner/out segments, along with DAPI (blue)

666 to label cell nuclei in eyes at 1 month (A,F,K,P,U), 2 months (B,G,L,Q,V), and 3 months
667 (C,H,M,R,W) after high-dose or low-dose (D,I,N,S,X) suprachoroidal AAV8 injections, as
668 compared to uninjected control eyes (E,J,O,T,V). Abbreviations: GCL, ganglion cell layers; INL,
669 inner nuclear layer; ONL, outer nuclear layer; RPE, retinal pigment epithelium. Scale bars: 100µm.

670

671 **[Figure 3]** B cell-mediated humoral immune responses against AAV8 and GFP after
672 suprachoroidal injections in NHP eyes. **(A-B)** Line plots compare serum anti-AAV8 antibody (A)
673 and anti-GFP antibody (B) levels in rhesus macaques before and after bilateral suprachoroidal
674 (SC/SC), suprachoroidal / subretinal (SC/SR), or bilateral intravitreal (IVT/IVT) AAV8 injections.
675 **(C)** Bar graphs show flow cytometry analysis of plasma B-cells with expansion upon GFP peptide
676 stimulation from PBMCs collected at various time points after high-dose suprachoroidal AAV8
677 injections into both eyes in Rhesus 02.

678

679 **[Figure 4]** T cell-mediated immune responses against AAV8 and GFP after suprachoroidal
680 injection. **(A-B)** Line plots compare IFN-γ-producing T-cell response against AAV8 capsid (A)
681 and GFP transgene (B) in peripheral blood mononuclear cells (PBMCs) before and after bilateral
682 suprachoroidal (SC/SC), suprachoroidal / subretinal (SC/SR), or bilateral intravitreal (IVT/IVT)
683 AAV8 injections. **(C-D)** Bar plots compare IFN-γ-producing T-cell response against AAV8 capsid
684 (C) and GFP transgene (D) from splenocytes collected at necropsy, as indicated by the
685 corresponding colored arrows for each animal. Abbreviations: SFU, spot-forming units; IFN-γ,
686 interferon gamma

687

688 **[Figure 5]** Systemic biodistribution of AAV8 after suprachoroidal injections. Bar graphs show
689 quantification of virally-encoded GFP genome copies measured from peripheral organs including
690 spleen, liver and kidney that were collected at the time of necropsy. Abbreviations: ND, not
691 detected; IVT, intravitreal; SC, suprachoroidal; SR, subretinal.

692

693 **[Supplementary Table 1]** Summary of study animals, demographic, injection mode, dose and
694 necropsy dates. Abbreviations: OD, right eye; OS, left eye; IVT, intravitreal; SC, suprachoroidal;
695 SR, subretinal; vg, viral genomes

696

697 **[Supplementary Figure 1]** Flow cytometry gating strategy for plasma B-cell quantification.

698

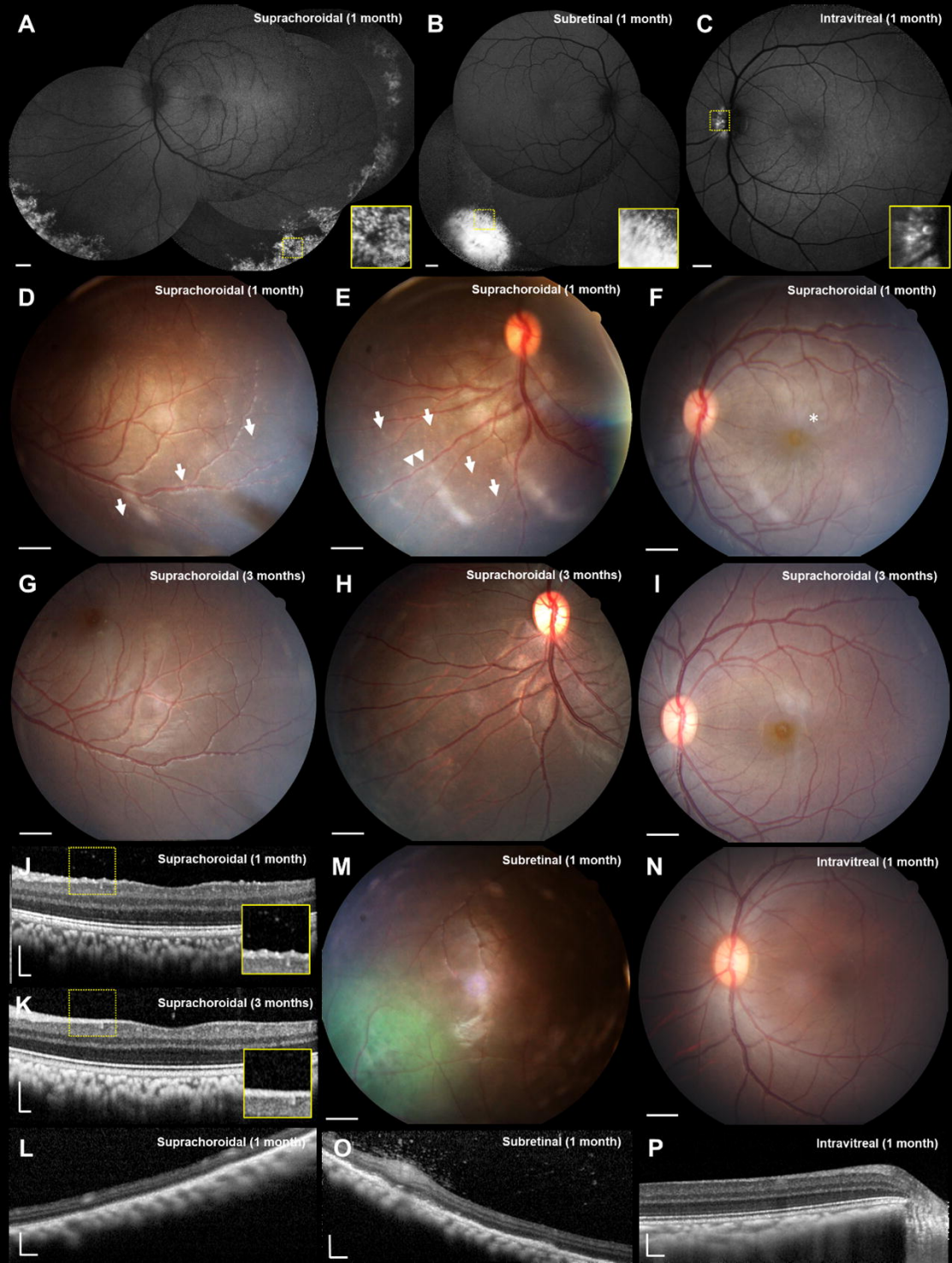
A
Suprachoroidal (1 month)
B
Subretinal (1 month)
C
Intravitreal (1 month)
D
Suprachoroidal (1 month)
E
Suprachoroidal (1 month)
F
Suprachoroidal (1 month)
G
Suprachoroidal (3 months)
H
Suprachoroidal (3 months)
I
Suprachoroidal (3 months)
J
Suprachoroidal (1 month)
K
Suprachoroidal (3 months)
M
Subretinal (1 month)
N
Intravitreal (1 month)
L
Suprachoroidal (1 month)
O
Subretinal (1 month)
P
Intravitreal (1 month)

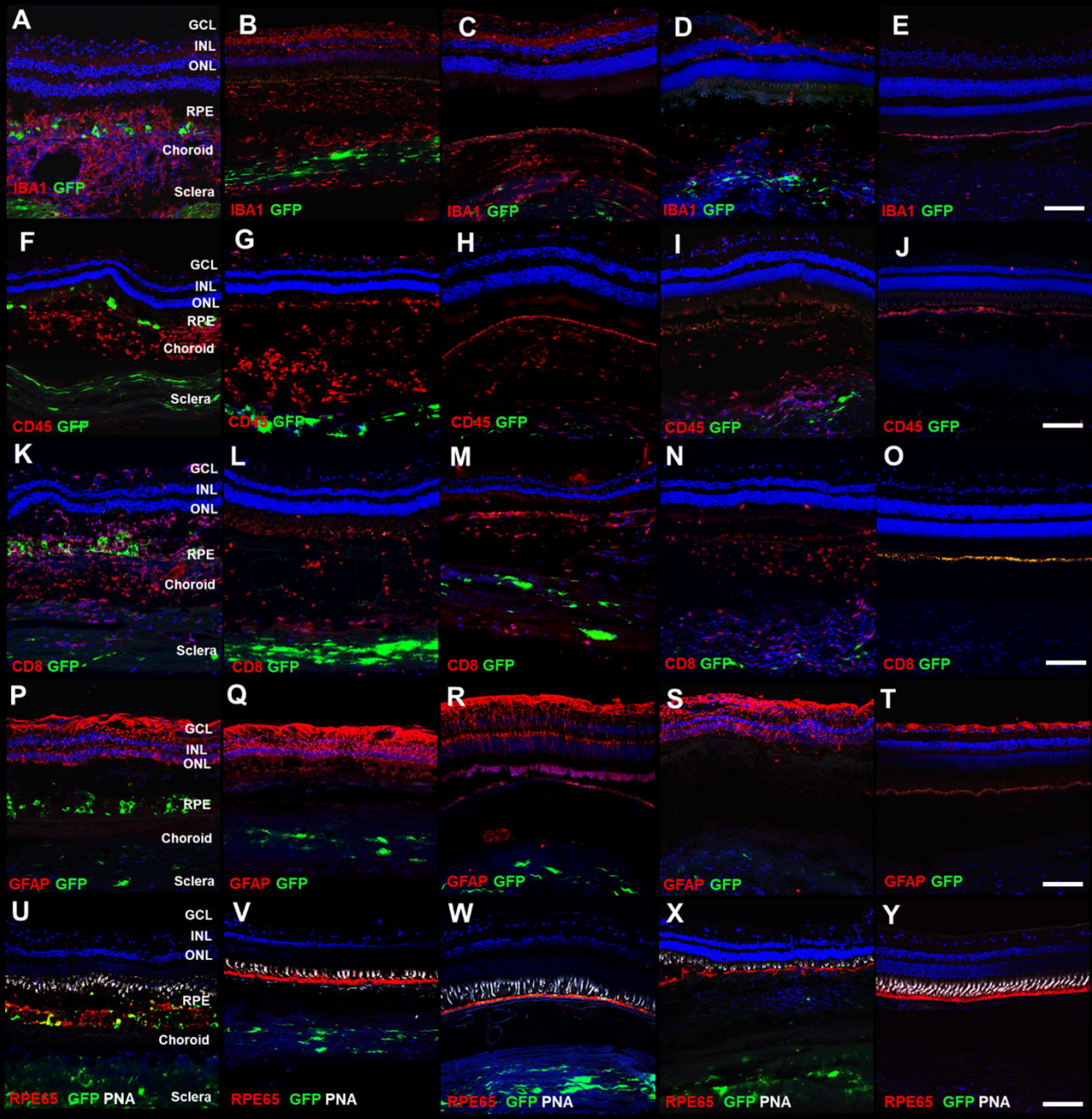
A
GCL
INL
ONL
RPE
Choroid
Sclera
IBA1 GFP
B
IBA1 GFP
C
IBA1 GFP
D
IBA1 GFP
E
IBA1 GFP
F
GCL
INL
ONL
RPE
Choroid
Sclera
CD45 GFP
G
CD45 GFP
H
CD45 GFP
I
CD45 GFP
J
CD45 GFP
K
GCL
INL
ONL
RPE
Choroid
Sclera
CD8 GFP
L
CD8 GFP
M
CD8 GFP
N
CD8 GFP
O
CD8 GFP
P
GCL
INL
ONL
RPE
Choroid
Sclera
GFAP GFP
Q
GFAP GFP
R
GFAP GFP
S
GFAP GFP
T
GFAP GFP
U
GCL
INL
ONL
RPE
Choroid
Sclera
RPE65 GFP PNA
V
RPE65 GFP PNA
W
RPE65 GFP PNA
X
RPE65 GFP PNA
Y
RPE65 GFP PNA

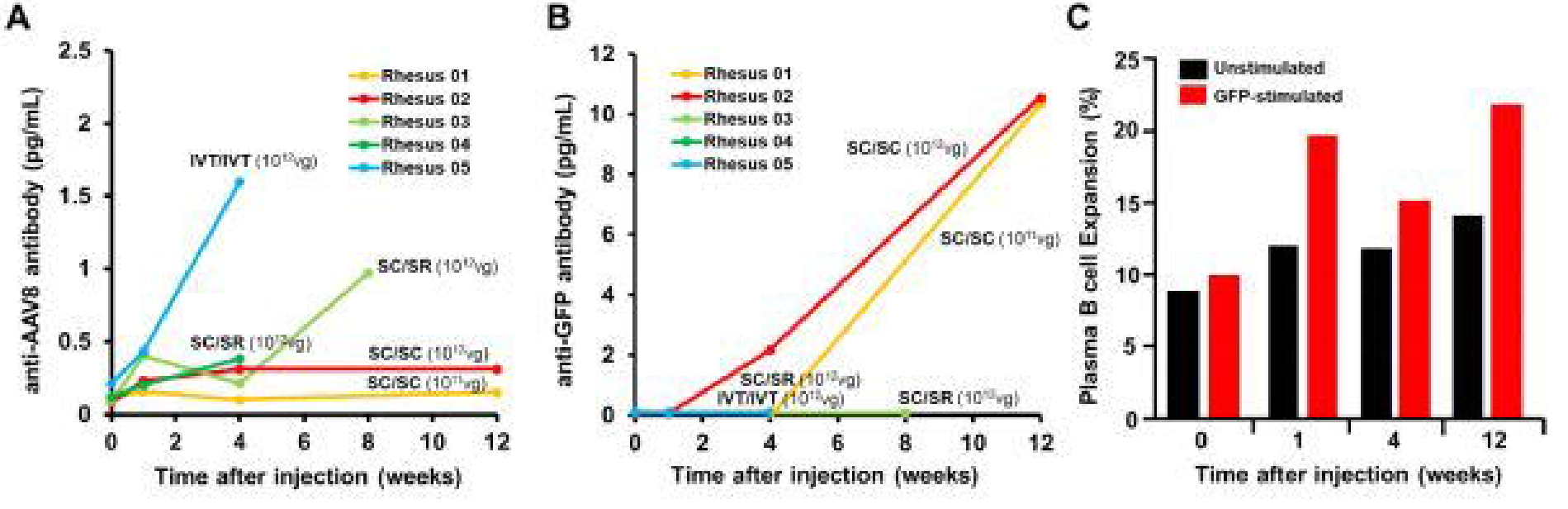
A
anti-AAV8 antibody (pg/mL)
2.5
2
1.5
1
0.5
0
Rhesus 01
Rhesus 02
Rhesus 03
Rhesus 04
Rhesus 05
IVT/IVT (10^{13}vg)
SC/SR (10^{13}vg)
SC/SR (10^{12}vg)
SC/SC (10^{13}vg)
SC/SC (10^{11}vg)
0 2 4 6 8 10 12
Time after injection (weeks)
B
anti-GFP antibody (pg/mL)
12
10
8
6
4
2
0
Rhesus 01
Rhesus 02
Rhesus 03
Rhesus 04
Rhesus 05
SC/SC (10^{13}vg)
SC/SC (10^{11}vg)
SC/SR (10^{13}vg)
IVT/IVT (10^{13}vg)
SC/SR (10^{11}vg)
0 2 4 6 8 10 12
Time after injection (weeks)
C
Plasma B cell Expansion (%)
25
20
15
10
5
0
Unstimulated
GFP-stimulated
0 1 4 12
Time after injection (weeks)

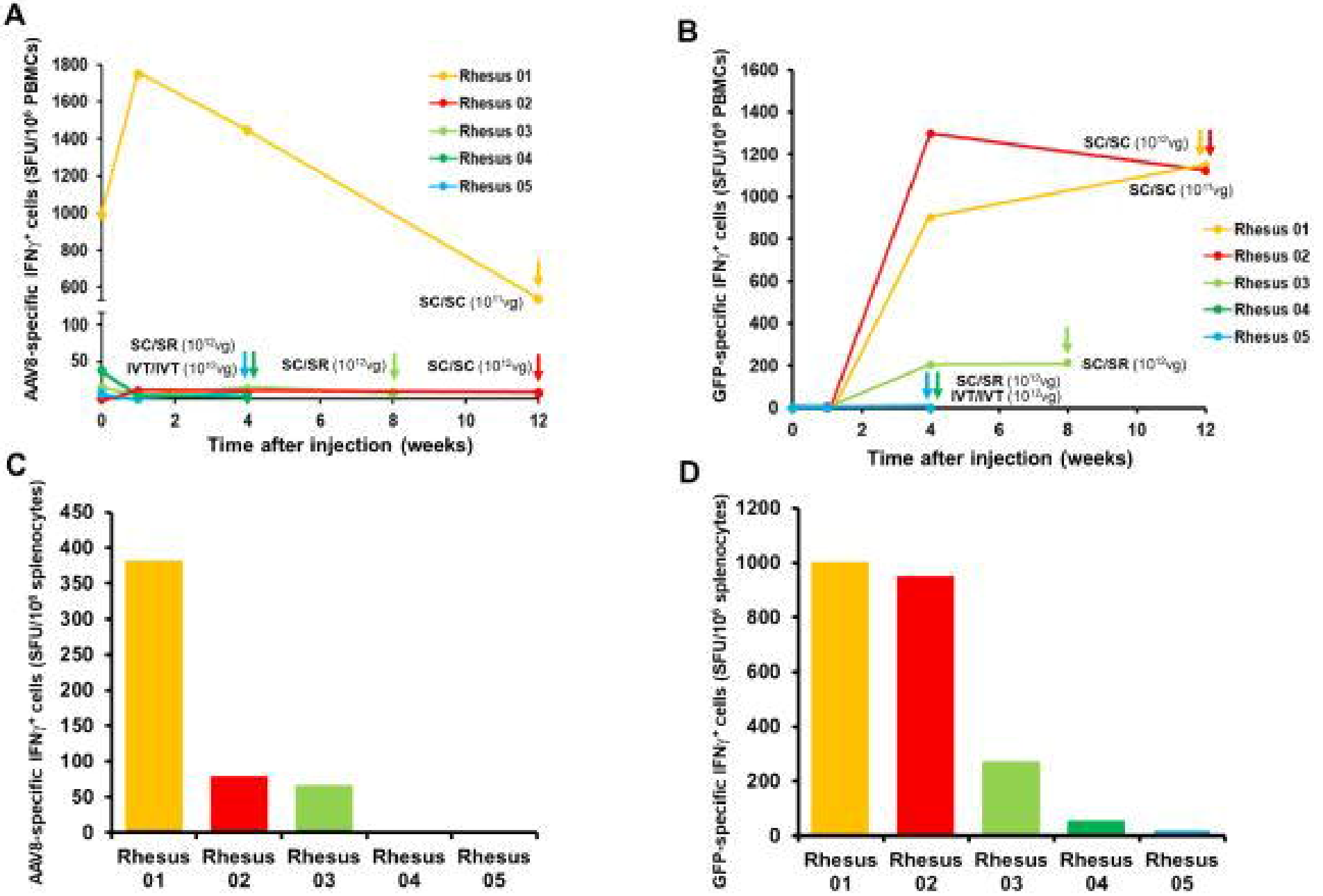
A
AAV8-specific IFNγ+ cells (SFU/10^6 PBMCs)
1800
1600
1400
1200
1000
800
600
100
50
Rhesus 01
Rhesus 02
Rhesus 03
Rhesus 04
Rhesus 05
SC/SC (10^11vg)
SC/SR (10^12vg)
IVT/IVT (10^12vg)
SC/SR (10^12vg)
SC/SC (10^12vg)
0
2
4
6
8
10
12
Time after injection (weeks)
B
GFP-specific IFNγ+ cells (SFU/10^6 PBMCs)
1600
1400
1200
1000
800
600
400
200
0
SC/SC (10^12vg)
SC/SC (10^11vg)
Rhesus 01
Rhesus 02
Rhesus 03
Rhesus 04
Rhesus 05
SC/SR (10^12vg)
SC/SR (10^12vg)
IVT/IVT (10^12vg)
0
2
4
6
8
10
12
Time after injection (weeks)
C
AAV8-specific IFNγ+ cells (SFU/10^6 splenocytes)
450
400
350
300
250
200
150
100
50
0
Rhesus 01
Rhesus 02
Rhesus 03
Rhesus 04
Rhesus 05
D
GFP-specific IFNγ+ cells (SFU/10^6 splenocytes)
1200
1000
800
600
400
200
0
Rhesus 01
Rhesus 02
Rhesus 03
Rhesus 04
Rhesus 05

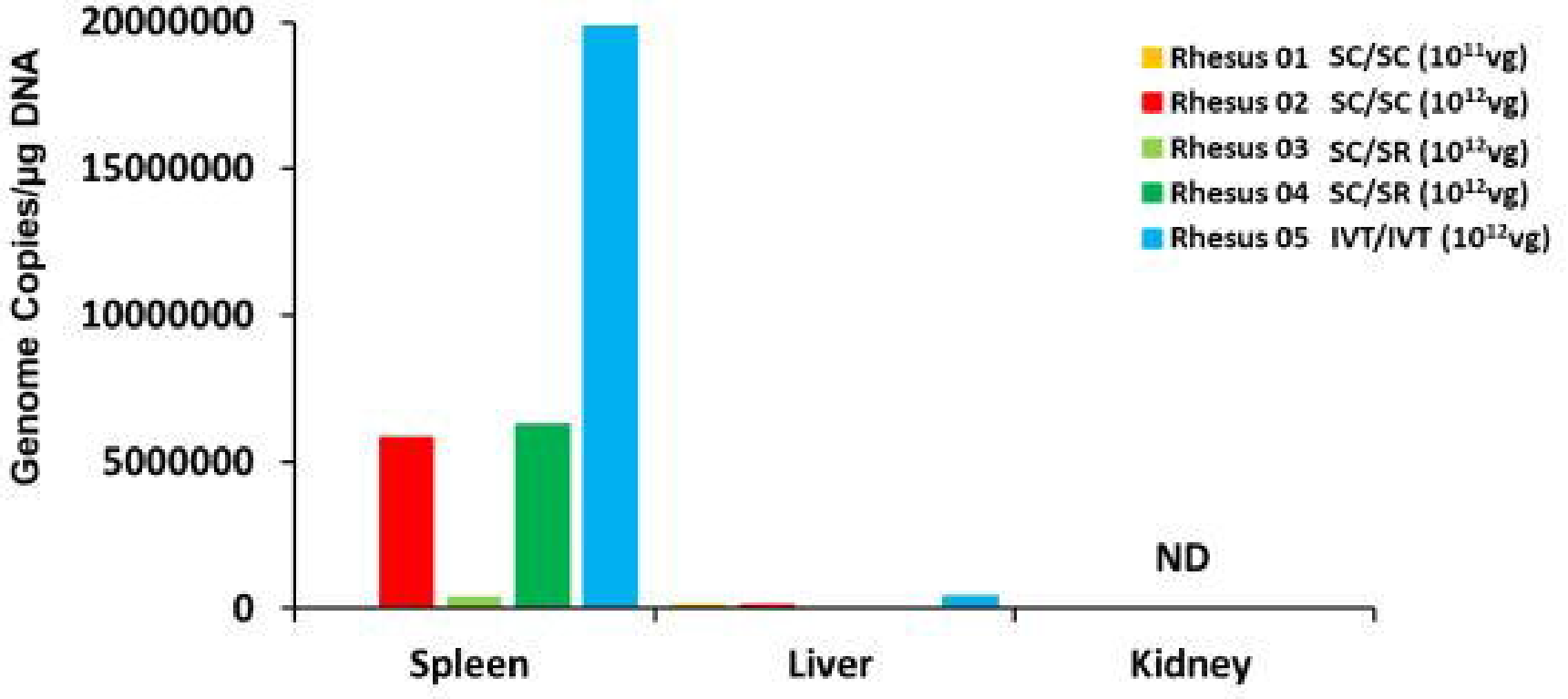
Genome Copies/µg DNA
20000000
15000000
10000000
5000000
0
Rhesus 01 SC/SC (10^11vg)
Rhesus 02 SC/SC (10^12vg)
Rhesus 03 SC/SR (10^12vg)
Rhesus 04 SC/SR (10^12vg)
Rhesus 05 IVT/IVT (10^12vg)
ND
Spleen
Liver
Kidney